NASA DEVELOP National Program
Georgia – Athens

Spring 2024

Platte River Water Resources

Assessing Urban Flood Vulnerability to Select Restoration Sites for Urban Woods and Prairies in the Great Plains

DEVELOP Technical Report
March 29th, 2024

Jennifer Mathis (Project Lead)
Jackie Encinas
Olivia Kirkland
Emma Vail

Advisor:
Dr. Marguerite Madden, University of Georgia, Center for Geospatial Research (Science Advisor)

Fellow:
Megan Rich (Georgia - Athens)

1. Abstract

In the Platte River Basin, wetlands provide ecosystem services such as flood mitigation and wildlife habitat. However, increasing urban development in the area has impacted natural floodplain processes, leading to a decline in wildlife habitat and an elevated flood risk for nearby communities. To address this issue, Audubon Great Plains' Urban Woods and Prairies (UWP) Initiative focuses on restoring vital habitats within urban areas to protect bird species and reduce flood hazards. Our project used remotely sensed data, including Landsat 8 Operational Land Imagery (OLI), Sentinel-2 Multispectral Instrument (MSI), and Sentinel-1 Synthetic Aperture Radar (SAR), to assess land use and land cover from 2013 to 2023, as well as flood extent. Broad-scale analysis of the land use land cover (LULC) showed some changes in land use patterns across the Central Platte River Basin, with the most notable being a decrease in Agricultural land coverage and an increase in Vegetation and Grassland coverage. Land use changes varied across 13 focal cities across the entire basin. In particular, developed land in Grand Island, NE, nearly tripled from 2019 to 2023, making it a good possible candidate for restoration efforts. We overlaid a flood extent map with the LULC classifications in Grand Island to identify possible restoration sites under UWP. This data will inform Audubon Great Plains in identifying potential restoration sites in key cities.

Key Terms

Platte River, land use land cover change, time series analysis, flood extent, HYDRAFloods, random forest classification

2. Introduction

2.1 Background Information

The Platte River Basin is one of the most prominent waterway systems in the United States Great Plains. The basin consists of two tributaries, the North and South Platte Rivers, originating in Colorado and flowing through Wyoming and Nebraska (Figure 1). The central stretch of the Platte River spans 310 miles to the eastern border of Nebraska, where it flows into the Missouri River (Birge et al., 2018). The basin's drainage area captures nearly 90,000 square miles (about the area of Colorado), and periodic flooding recharges essential wetlands for fish and wildlife (Birge et al., 2018). Wetlands offer ecosystem services like water filtration, carbon storage, and flood mitigation (Audubon Great Plains, 2023a). Wetlands serve as natural buffers, slowing water flow and retaining water within the floodplain.

Over time, the Platte River Basin landscape has experienced significant transformations. The conversion of natural areas to agricultural & urban land use increases the demand for water supply from the river. The expansion of urban regions into floodplains and the proliferation of impervious surfaces have led to the degradation and loss of wetlands, compromising their ecological function (Dewan & Yamaguchi, 2009). Additionally, alterations to river flow caused by dams and reservoirs impact critical habitats for threatened and endangered bird species like the Whooping Crane and Piping Plover (Audubon Great Plains, 2023b).

Climate shifts are expected to impact communities and intensify flood events in the basin. The Fourth National Climate Assessment predicts temperature rises, prolonged droughts, and increased frequency of heavy precipitation events in the Great Plains, all of which can have compounding effects on the basin (Conant et al., 2018). For example, warmer temperatures and earlier snowmelt can affect water resources and degrade habitat quality (Birge et al., 2018). In March 2019, the US Mid-West experienced a record-breaking snow-flood event driven by rain-on-snow, warm temperatures, and snowmelt, devastating the region (Velasquez et al., 2023). Mitigation efforts, like green infrastructure, green spaces, and other "nature-based solutions," can help rural and urban communities and ecosystems adapt to changing climatic events (Kabisch et al., 2016).

2.2 Project Partners and Objectives

Audubon Great Plains (AGP) is a regional office of the National Audubon Society serving Nebraska, North Dakota, and South Dakota. AGP's mission is to protect birds and improve and restore bird habitat while

engaging the communities it serves. A key strategy for restoration is Audubon Great Plains' Urban Woods and Prairies (UWP) Initiative – a partnership between Audubon Society and local landowner entities aimed at restoring and enhancing riparian grassland, wetland, and woodland habitats to benefit local communities and wildlife (Audubon Great Plains, 2023c). UWP selects sites in urban areas where nature-based solutions like green infrastructure are needed the most to mitigate flooding impacts to communities while providing habitat for bird species, recreational opportunities, and improving habitat connectivity.

Our project used Earth observations to assess land use land cover (LULC) changes and flood extent in springtime (as this was the local flood season identified by partners) from 2013 to 2023, assisting Audubon Great Plains in pinpointing restoration sites in cities within the Platte River Basin as part of the UWP Initiative. While AGP is skilled at employing GIS tools to analyze species dispersal and habitat connectivity, integrating remote sensing techniques into their decision-making process is a new endeavor. With consideration to partner input, we focused on thirteen cities within the Platte River Basin: Casper, WY; Torrington, WY; Fort Morgan, CO; Brush, CO; Sterling, CO; Scottsbluff, NE; Schuyler, NE; Columbus, NE; Plattsmouth, NE; Lincoln, NE; Grand Island, NE; North Platte, NE; and Freemont, NE (Figure 1). The selection was based on proximity to the Platte River, large populations, and existing local partnerships.

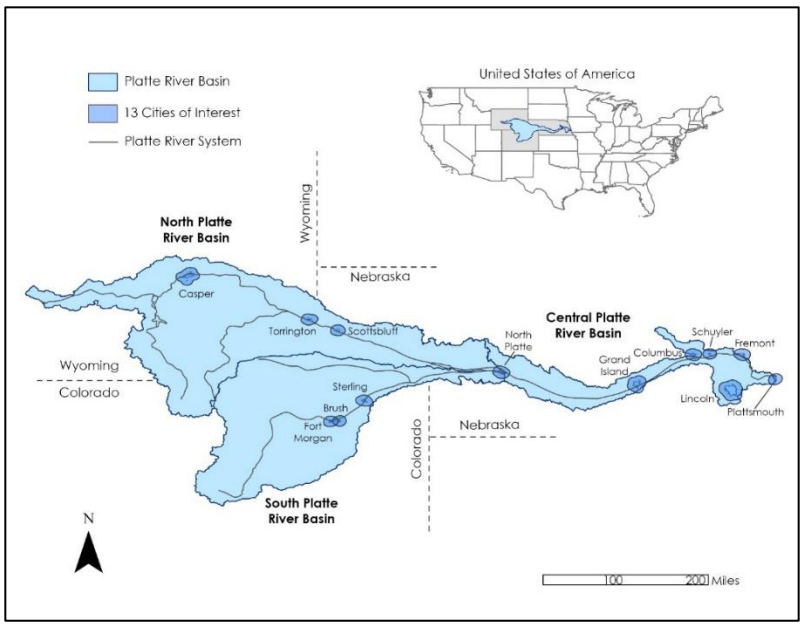

Figure 1. Map showing the study areas within the Platte River Basin.

Past studies provided a foundation for our approach to assessing LULC change and flood extent. Dewan & Yamaguchi (2009) used Landsat MSS, TM, and ETM+ imagery and a supervised classification algorithm to quantify urbanization in Bangladesh from 1975 to 2003. We followed a similar methodology using Landsat OLI and a machine learning classification to classify land cover. Williams et al. (2021) and Chittumuri et al. (2022) used optical and SAR imagery and HYDRAFloods, an open-source Python application developed by NASA SERVIR, to visualize flood extent in Central America and Coastal Georgia following a natural disaster event. We replicated the HYDRAFloods workflow, using only SAR imagery, to map the extent of the floods in March 2019.

3. Methodology

This study presents a comprehensive methodology for assessing LULC changes and associated impacts within the Platte River Basin. The steps taken are broken down into the following three separate but

inherently connected components. 1) Leveraging Landsat 8 imagery, we employed a random forest classification approach to delineate LULC classes. Additionally, we assessed urbanization and flooding impacts on partner-identified highly impacted cities using Sentinel-2 satellite imagery. The machine learning process includes data acquisition, preprocessing, feature selection, training data collection, model training, and evaluation. 2) Additionally, we conducted a Normalized Difference Vegetation Index (NDVI) analysis to elucidate the effects of major flood events on critical vegetation areas that the UWP initiative could use to identify restoration sites. 3) Finally, we performed flood risk mapping and overlayed the assessment with the classified LULC to quantify the land cover types affected by flooding. This provided insights into the dynamics between LULC changes and flood risks in the region.

3.1 Data Acquisition

3.1.1 LULC Classification

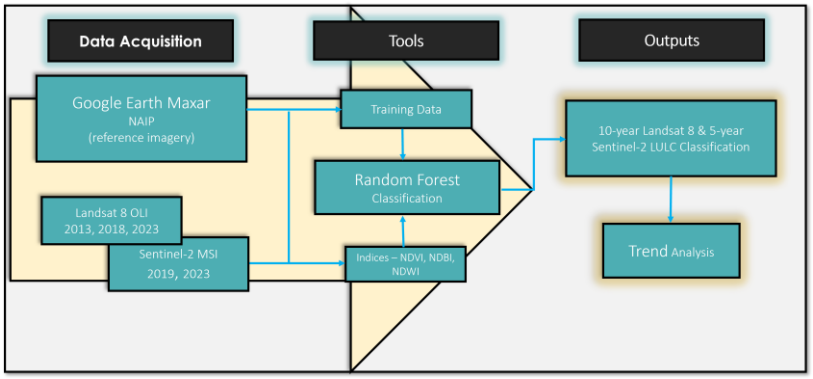

Figure 2. Flowchart depicting the overall methodology for the LULC classification analysis.

Our study employed Landsat 8 OLI and Sentinel-2 MSI imagery. We sourced the imagery from the Google Earth Engine (GEE) platform. This selection of datasets ensured comprehensive coverage and a broad range of spectral information essential for conducting a random forest classification analysis and mapping flood extent.

To facilitate land cover classification, we leveraged reference datasets from the United States Geological Survey's (USGS) National Land Cover Database (NLCD) and aerial imagery sourced from the United States Department of Agriculture's (USDA) National Agriculture Imagery Program (NAIP) via the GEE platform. Additionally, we incorporated Google Earth Basemap imagery (originally sourced from Maxar Worldview 3), which had already been upsampled and processed through super-resolution algorithms within the GEE platform, to augment our training data with high-resolution spatial information (Table 2).

Table 1.
Earth observation satellites and sensors, parameters, and image capture dates.

Platform / Sensor	Parameters	Processing Level	Image Capture Date	GEE Asset ID
Landsat 8 OLI	RGB True Color, NDVI, Normalized Difference Built-up Index (NDBI), and Normalized Difference Water Index (NDWI)	Level 2	Spring (April 1 – June 30) 2013 – 2023	LANDSAT/LC08/C02/T1_L2

Sentinel-2 MSI	RGB True Color, NDVI, NDBI, and NDWI	Level 2-A	Spring (April 1 – June 30) 2013 – 2023	COPERNICUS/S2_SR_HARMONIZED

Table 2.
Ancillary datasets

Name	Year	Source	Spatial Resolution	Use
NLCD	2021	USGS	30-meter	Reference for LULC Training Data
NAIP	2019	USDA	1-meter	Reference for LULC Training Data
Basemap Imagery	N/A	GEE	0.6-meter	Reference for LULC Training Data

3.1.2 Flood Risk Mapping and LULC Overlay Assessment

We performed a land type and flood extent overlay assessment to evaluate the impact of flooding events on different land types within the basin. This assessment quantified the extent of flooding across various land cover classes, aiding in the identification of vulnerable areas susceptible to inundation. Figure 3 illustrates an overview of the steps taken to produce a flood extent map at the city level.

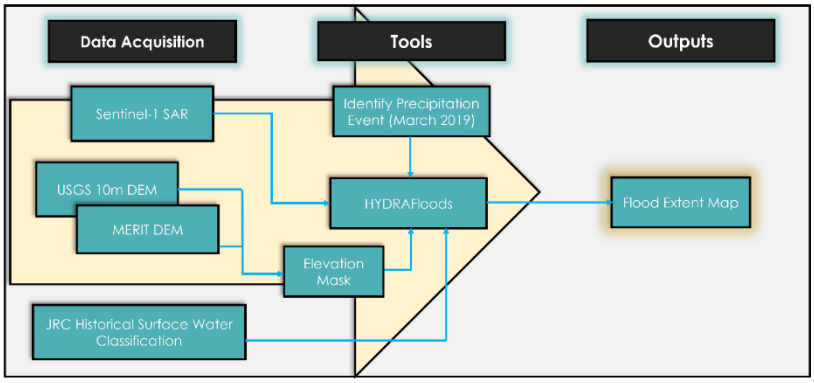

Figure 3. Flowchart depicting flood extent map methodology.

To generate our flood extent map, we leveraged Sentinel-1 SAR imagery sourced from the GEE platform and Digital Elevation Models (DEMs) sourced from USGS and the Multi-Error-Removed Improved-Terrain (MERIT) Hydro dataset. These DEMs served as foundational elevation datasets crucial for flood modeling. To delineate permanent water bodies, we referenced the Joint Research Centre (JRC) Historical Surface Water Classification dataset. All data was acquired through the HYDRAFloods package on Google Collaboratory (Collab). We conducted Sentinel-1 SAR image processing utilizing HYDRAFloods within the Google Collab environment. The temporal scope of this analysis was defined between March 1 and March 21, 2019, aiming to capture the peak of flooding activity around March 14, 2019. This period was selected to optimize the selection of available Sentinel-1 SAR imagery based on pixel count that fell within the bounds of our study area, ensuring the successful execution of HYDRAFloods by excluding scenes with insufficient pixel coverage.

Table 3.
Earth observation satellites and sensors, parameters, and image capture dates.

Platform / Sensor	Parameters	Processing Level	Image Capture Date	GEE Asset ID
Sentinel-1 C-SAR	Backscatter	Level 1	March 1-21, 2019	COPERNICUS/S1_GRD

Table 4.
Ancillary datasets

Name	Source	Use
JRC Historical Surface Water Classification	European Commission JRC	Permanent surface water classification for HYDRAFloods
USGS 3DEP 10m DEM	USGS	Elevation information for HYDRAFloods
MERIT Hydro 90m DEM	Dai Yamazaki (University of Tokyo)	Hydrological flow and elevation information for HYDRAFloods

3.2 Data Processing

3.2.1 LULC Random Forrest Classification

We processed Landsat 8 and Sentinel-2 satellite imagery within the GEE platform. We clipped the imagery to our study areas and temporally filtered it to encompass the months from April through July, covering the years 2013 to 2023. This time frame selection aimed to accommodate seasonal variations and capture vegetation growth at its peak. Specifically, Sentinel-2 imagery was available for the years 2019 through 2023. We applied a cloud mask of 35% and 20%, capturing the minimal percentage of cloud cover feasible for both Landsat 8 and Sentinel-2 imagery and intersecting with our study area boundaries. Finally, we calculated a median 8-band multispectral image for each year to be analyzed in the time series analysis and combined it to create a single RGB true color composite image for the Central Platte Basin and 13 focal cities.

Relevant spectral indices from the satellite imagery were derived from the satellite imagery, such as NDVI (Eq. 1), NDWI (Eq. 2), and NDBI (Eq. 3).

Eq. 1) $$NDVI = \frac{(NIR-RED)}{(NIR+RED)}$$ (Rouse et al. 1974)

Eq. 2) $$NDWI = \frac{(GREEN-NIR)}{(GREEN+NIR)}$$ (Gao 1996)

Eq. 3) $$NDBI = \frac{(SWIR-NIR)}{(SWIR+NIR)}$$ (Zha, Gao, and Ni 2003)

We generated point training data within the GEE platform. During the sampling phase, Landsat 8 and Sentinel-2 imagery were utilized alongside reference datasets such as Worldview-3 integrated into the GEE platform, NAIP imagery, and NLCD data to ensure robustness in the training data formulation process. For the Central Platte Basin study region, we extracted training data from Landsat 8 imagery for the years 2013, 2018, and 2023. We characterized four primary LULC classes: open water, developed, agriculture, and mixed vegetation and grassland. We generated 800 points per year, with 200 points per class. We then sampled these point data across the land, ensuring they were evenly distributed for machine learning classification. We employed Sentinel-2 imagery to generate training data for the 13 focal cities in 2019 and 2023. We identified five distinct LULC classes: open water, barren land, developed, agriculture, and mixed forest and wetland. We created 6,500 training points for each year, with 500 points per class. We uniformly allocated points among cities and distributed them across urban landscapes to ensure comprehensive coverage of diverse features.

Random forest is an ensemble machine learning algorithm that implements multiple decision trees during dataset training to make predictions (Breiman, 2001). Tree construction and feature selection revolve around randomness to reduce overfitting and improve accuracy. The random forest algorithm is commonly used for classification and regression tasks. Within GEE, the random forest algorithm was utilized to classify our areas of interest, employing 1,000 decision trees to train the algorithm. Additionally, spectral indices such as NDVI, NDWI, and NDBI were included as input to augment the accuracy of vegetation, water, and developed area delineation and identification.

3.2.2 NDVI Analysis

In addition to using NDVI in our random forest classification, we also used our NDVI mean of 10 years, September through November, to view each city of interest. This allowed us to identify areas within the cities that are constantly impervious and, therefore, more ideal candidates for implementing green infrastructure. We used GEE to calculate the seasonal NDVI (Eq. 1) of the study area for 2013 through 2023. We obtained Landsat 8 imagery and applied a cloud mask to exclude images with more than 20% cloud cover. Our team selected spring imagery between March and May and fall between September and November. We merged each season of imagery to create a single image collection and calculated the mean NDVI for each season over the study period.

3.2.3 HYDRAFloods Model Execution

Subsequently, we employed a gamma Maximum a posteriori (MAP) filter to reduce the granular appearance inherent in SAR imagery. Elevation data derived from the USGS 3D Elevation Program (3DEP) 10-meter DEM provided an angular-based radiometric slope correction method (Vollrath et al., 2020). This correction accounted for backscatter effects and removed shadows exceeding a 10-meter height threshold from the SAR image. We then used the MERIT Hydro elevation dataset (Yamazaki et al., 2019) to extract the Height Above the Nearest Drainage (HAND) band, masking regions exceeding 20 meters above the nearest water body. Following this, we incorporated the Edge Otsu thresholding algorithm to delineate between water and non-water pixels (Markert et al., 2020). Lastly, we employed the JRC Yearly Water Classification History dataset (Pekel et al., 2016) to discriminate permanent surface water features and flooded water areas.

3.3 Data Analysis – LULC Classification

We performed an accuracy assessment using a confusion matrix, wherein we partitioned the training data into two random fractions – one used for training and the other for validation – for a robust comparison. Metrics included overall accuracy, producer's accuracy, and consumer's accuracy, which were computed to evaluate the classification performance comprehensively. The emphasized measure of accuracy, overall accuracy, quantifies the proportion of correctly classified samples in the dataset and serves as a general measure of the classifier's performance across all classes. Following the computation of overall accuracy assessments for the Landsat-8 and Sentinel-2 study areas, average overall accuracy was calculated for both the central basin (2013-2023) and the 13 focal cities (2019-2023) classifications.

4. Results & Discussion

4.1 Analysis of Results

This section presents a detailed examination of LULC dynamics within the Central Platte Basin, utilizing remote sensing datasets and advanced analytical methodologies. The analysis encompassed broad-scale and city-scale assessments, accuracy evaluations, flood extent overlay assessment, NDVI analysis, LULC time series, and flood extent mapping. The findings contribute to our knowledge of landscape changes and provide valuable insights for informed decision-making in land management and environmental restoration efforts implemented by the UWP initiative.

4.1.1 Broad-scale analysis of general LULC trends and accuracy of the Central Platte Basin using Landsat-8 OLI MS

Using Landsat 8 OLI imagery, a broad-scale analysis of general LULC trends and accuracy within the Central Platte Basin provided insights into the spatial distribution and temporal changes of land cover across the

basin, facilitating the understanding of large-scale landscape dynamics. The Central Basin LULC time series analysis showed preliminary, general variation in land type from 2013 to 2023 (Figure 4). Agriculture decreased from 57.3% of total land coverage to 49.9%, while Vegetation and Grasslands increased in coverage from 30.4% to 39.8%. Open Water decreased, accounting for 6.6% and 5.4% of land type in 2013 and 2023, respectively, while Developed land remained relatively unchanged (5.6% and 5%). In 2018, we observed a spike in Developed land, accounting for 10.7% of land type. The spike is likely a result of misclassifications due to the large spatial resolution of Landsat 8 and similar spectral signatures between land type classes. This holds particularly true for Agriculture and Grasslands, where fallow agriculture lands were inaccurately categorized as grassland, resulting in an overestimation of the vegetation and grassland class. These statistics reflect classifications generated from the trained random forest algorithm; for the Landsat 8 classification, the average overall accuracy of the algorithm is 90.68%.

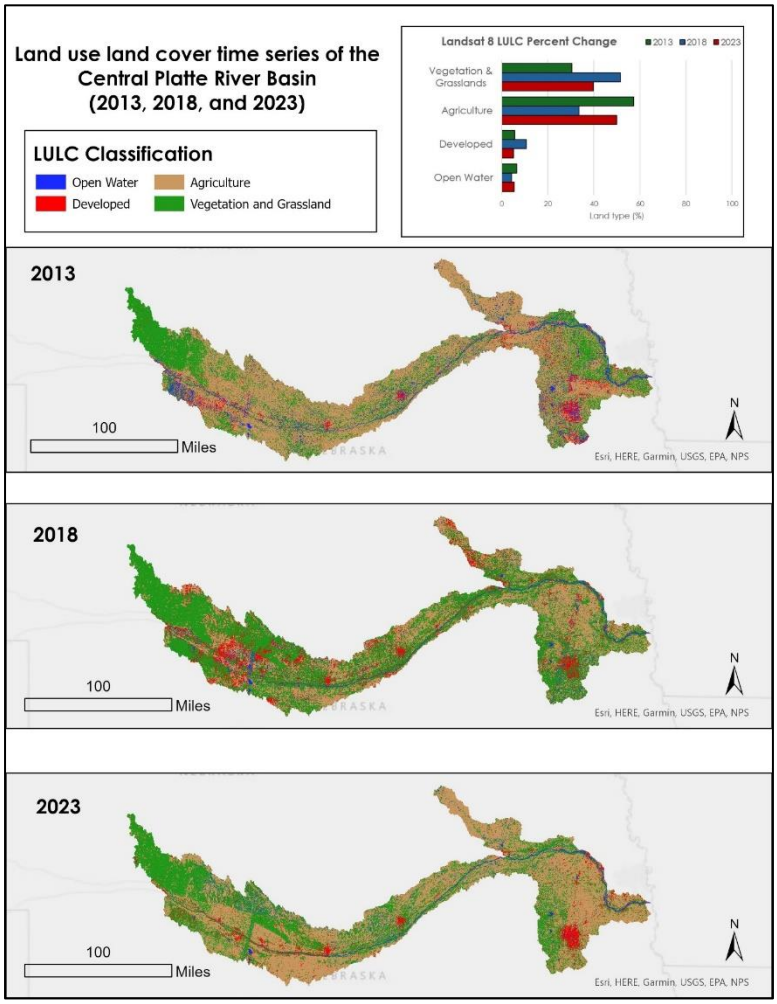

Figure 4. LULC Time Series of the Central Platte River Basin in 2013, 2018, and 2023.

Table 5.
Table of the LULC percent change for the Central Platte Basin 10-year time series.

	Open Water	Developed	Agriculture	Mixed Vegetation
% Change	-18.87%	-12.09%	-13%	+30.82%

4.1.2 City-scale analysis of general LULC trends and accuracy of the Central Platte Basin using Sentinel-2
The city-scale analysis employing Sentinel-2 MS data enabled a more detailed exploration of LULC trends within urban areas, followed by an accuracy assessment to ascertain their reliability in capturing LULC dynamics accurately. The LULC change detection in the 13 focal cities showed general land type variation in 2019 and 2023 (Figure A1, Table A1). Figure 3 depicts land type changes in three cities: Brush, CO; Grand Island, NE; and Torrington, WY. Agriculture and Grassland land type decreased in Grand Island (80.2% to 77.6%) and Torrington (91.6% to 84.5%) and increased in Brush (74.2% to 80.0%). Grand Island and Brush saw an increase in Developed land (1.8% to 4.9% and 7.4% to 8.1%, respectively). However, Torrington experienced a decrease in Developed land (5.3% to 4.7%). Barren land decreased in Brush (3.7% to 1.5%) and Grand Island (3.1% to 2.6%) and increased in Torrington (1.6% to 5.4%). Finally, Forests and Wetlands increased in Torrington (3.1% to 6.9%), decreased in Brush (13.6% to 9.2%), and remained relatively unchanged in Grand Island (11.7% and 11.8%). These statistics reflect classifications generated from the trained random forest algorithm; for the Sentinel-2 classification, the average overall accuracy of the algorithm is 93.2%. Although the Sentinel-2 imagery featured a higher spatial resolution at a 10-meter pixel size and increased LULC detail from our Central Basin scale, further refinement of the training data with ground truth data could improve the classification results.

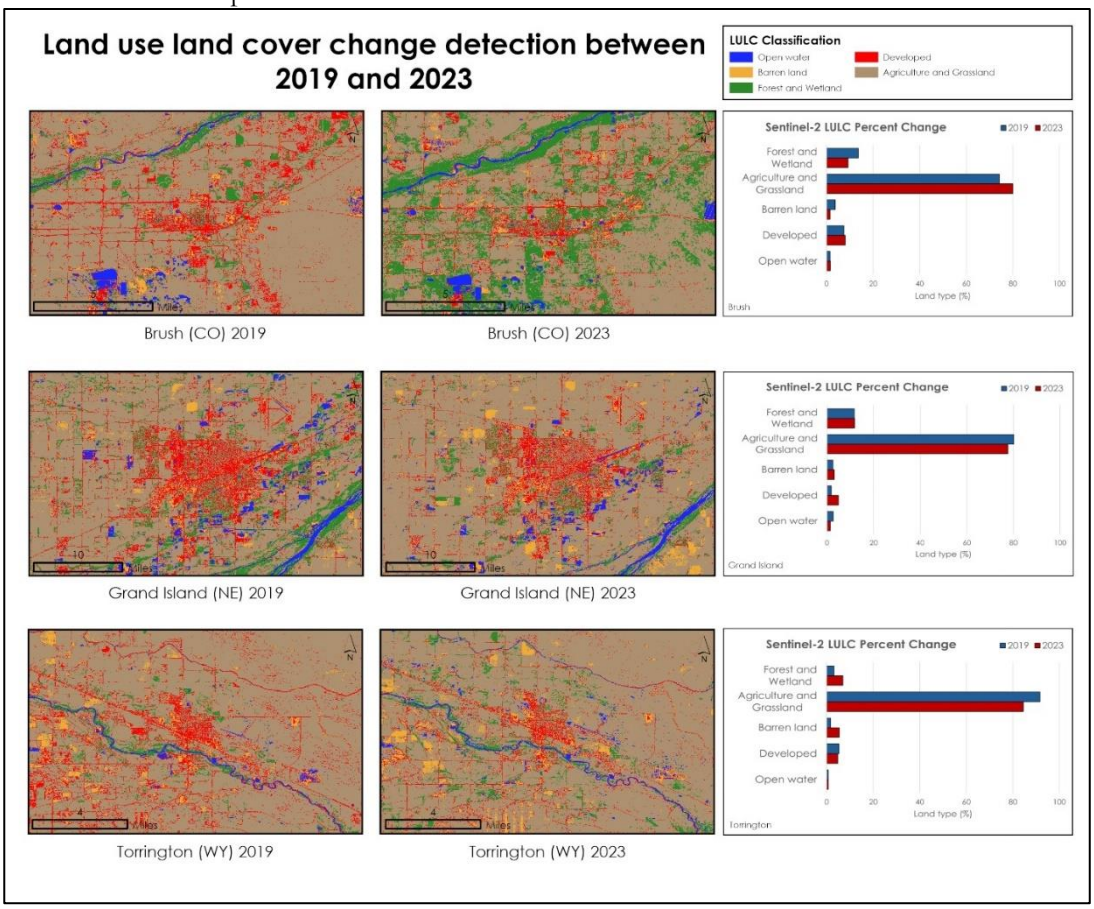

Figure 5. LULC change detection between 2019 and 2023 in Brush, CO; Grand Island, NE; Torrington, WY.

4.1.3 NDVI Analysis
Before the flooding event on March 14, 2019, the histogram Figure 6 (a) showed most pixels from -0.04 to 0.02, suggesting relatively sparse vegetation. NDVI values around 0 typically signify bare soil, urban areas (impervious surfaces), or areas with little to no vegetation. This sparse vegetation coverage could be due to urbanization, agriculture, or dry conditions before flooding. Following the flood event, the histogram (b)

peaks at around 0.2, suggesting a significant increase in vegetation cover compared to before the flooding event. This shift could be attributed to several factors. Floods often deposit nutrient-rich sediment onto the land, providing fertile soil for vegetation growth and leading to a rapid increase in vegetation density following the flooding. Additionally, floods also replenish soil moisture levels and may create favorable conditions for plant growth and germination. Consequently, vegetation that was previously sparse or dormant may start to thrive.

The gradual tapering of NDVI values towards 1 indicates ongoing growth and recovery post-flooding. While there has been an increase in vegetation density post-flooding, it might not have reached its full potential. The right-sided tapering toward 1 in the histogram Figure 6 (b) may indicate vegetation is in the process of regrowth and/or restoration. Overall, the transition in NDVI values from predominantly low values around 0 before the flooding event to higher values after the event might highlight a positive impact on vegetation health and density.

a).

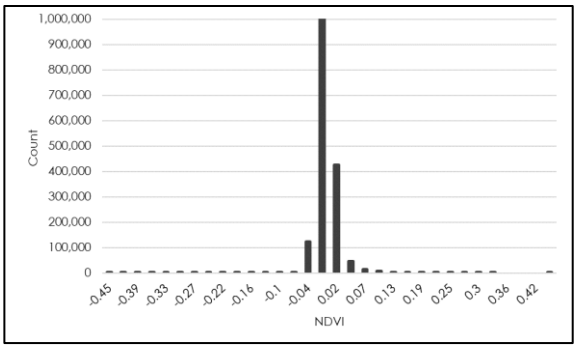

b).

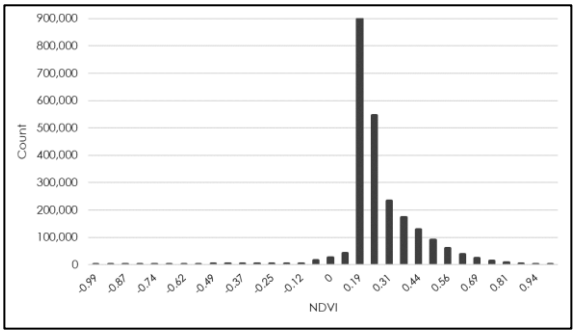

Figure 6. a): Calculated NDVI of Grand Island City, NE, before a flood event; b)Calculated NDVI of Grand Island City, NE, after the catastrophic March 14, 2019, flood event.

4.1.4 Land type and flood extent overlay assessment

We conducted a land type and flood extent overlay assessment to evaluate the impact of flooding events on different land types within the basin. This assessment quantified the extent of flooding across various land cover classes, aiding in the identification of vulnerable areas susceptible to inundation. The statistical analysis of overlay assessment revealed a statistical analysis of land-type areas after flooding in Grand Island in 2019. Results of the statistical analysis showed that 0.33% of Developed, 0.22% of Barren, and 0.87% of Forests and Wetland lands in Grand Island were inundated during the March 2019 flood event. Agriculture land had the highest percentage of area impacted by flooding, with 5.9% of agricultural lands covered by water.

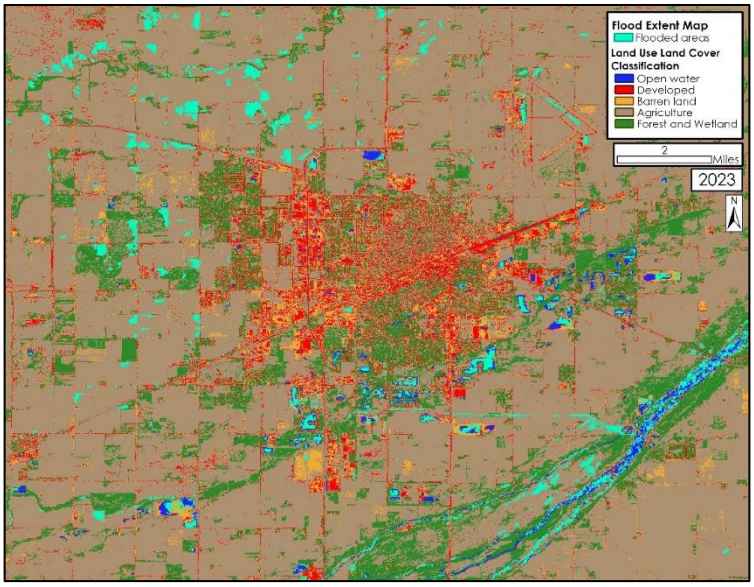

Figure 7. Map depicting an overlay of the Flood Extent Map and LULC: Grand Island Map.

4.2 Limitations and Feasibility for Partner Use

4.2.1 LULC Time Series

Our approach to creating the LULC time series analysis yielded several limitations. First, the extent of the Platte River Basin made it challenging to process Landsat 8 imagery in GEE. To account for this, we focused our efforts on 1) the Central Platte Basin for the 10-year LULC time series, using Landsat 8 imagery, and 2) the thirteen focal cities identified by the partner for the 5-year LULC change detection, using Sentinel-2 imagery. Second, the lack of field data, such as photographs or site visitation, made it difficult to confirm the accuracy during training data creation and in the resulting LULC classifications. We accounted for this limitation by incorporating reference imagery into our workflow. We used GEE Basemap Imagery, NLCD, and NAIP for visual verification while we created training data and compared our resulting LULC classifications. Third, the satellite imagery resolution of Landsat 8 (30 meters) and Sentinel-2 (10 meters) made it difficult to distinguish forests from riparian wetlands. We make recommendations for addressing this in the 4.3 Future Recommendations section. With additional time and resources, it is feasible to expand this scope to analyze more of the Platte River Basin and more focal cities using Landsat 8 and Sentinel-2 imagery.

4.2.2 Flood Extent Map

We encountered a variety of limitations in using HYDRAFloods to analyze flood risk. First, the spatial extent of the Platte River Basin made it challenging to process Sentinel-1 imagery in Google Collab. There was also a lack of Sentinel-1 SAR imagery available over the study region, which limited city selection. Additionally, because the purpose of the HYDRAFloods tool was to depict a single flooding event, the sparsity of imagery limited the selection of flooding events to evaluate. To account for this limitation, we focused on a single city – Grand Island, Nebraska – to establish our methodology and determine its feasibility. However, this method is easily replicable for additional cities. Finally, we lacked field data, such as photographs or site visitations, to verify the accuracy of the resulting flood extent map. In summary, we concluded that using HYDRAFloods to evaluate flood risk for the entire Platte River Basin is not feasible.

4.2.3 Summary

Despite these limitations, we produced the LULC time series and the Flood Extent Map in ten weeks. With additional time and resources, it is feasible to refine and expand the scope of the LULC classifications. However, due to the limitations of using HYDRAFloods, we recommend a different approach to analyzing flood risk.

4.3 Future Recommendations

The exploratory nature of our project allowed us to develop various recommendations for future work. There are ways to improve our current methods and incorporate additional tools into future research. Our recommendations are meant for consideration by our partner and future DEVELOP work.

1) LULC classification was feasible; however, we suggest that the partner spend more time refining training data for both Landsat 8 and Sentinel-2 LULC classifications if using a random forest classification method. Training data refinement will improve the accuracy of these classifications.
2) We recommend that future work should prioritize wetland identification using SAR, LiDAR, or National Wetland Inventory datasets. Wetland masking in classifications will ensure that wetlands are adequately delineated to provide the level of detail necessary for the partner's focus on wetland restoration.
3) We do not believe HYDRAFloods is a practical tool for our partners to conduct flood risk analysis for the entire Platte River Basin. HYDRAFloods is useful for mapping the extent of past floods; however, it may not be practical for mapping potential flood risk. We recommend that the partners evaluate flood risk using other tools like stormwater flow analysis. Alternative methods will create a more practical product for the partner to help implement green infrastructure.
4) Based on conversations with our partner, we recommend that a future DEVELOP team could incorporate an urban growth model in their work. Examining both historical and predicted change will ensure that the partner's proactive conservation efforts align with the evolving landscapes.

5. Conclusions

Our project served as a proof of concept for using a combination of Landsat 8 OLI and Sentinel-2 MSI observations to create a basin-scale and city-scale LULC time series and flood extent map of a focal city. Preliminary basin-scale LULC time series showed a general increase in Vegetation and Grassland, decreases in Open Water and Agriculture, and little change in Developed land types. There was variation in land cover change throughout all thirteen cities; however, we highlighted the changes observed in Brush, CO; Grand Island, NE; and Torrington, WY. From 2019 – 2023, Brush experienced an increase in Agriculture and Grassland, and Developed land types, while Torrington saw decreases in Agriculture and Grasslands, and Developed land. Based on our preliminary results, Grand Island saw an increase in developed land, while agriculture and grasslands decreased, making the city a good candidate for restoration efforts.

Misclassifications in the basin-scale LULC time series and city-scale LULC change detection are likely a result of the coarse resolution of satellite imagery coupled with confusion between spectral signatures of land type classes, specifically Agriculture and Developed. An overlay assessment of the high-resolution classifications with flood extent in Grand Island identified the land types most affected by the 2019 flood event: Agriculture and Grasslands, Forests and Wetlands, and Developed lands. The resulting flood map and overlay can help Audubon Great Plains' local outreach efforts to identify possible restoration sites for the Urban Woods and Prairies Initiative and lead to increased impact on community concerns (Figure 5).

Given Audubon Great Plains' goals of addressing flooding and wetland connectivity concerns, the LULC classifications and flood map are a good starting point for local outreach efforts to identify potential sites for restoration. We acknowledge the limitations of our study and offer several recommendations for future work that will improve the accuracy of the products and be more robust for Audubon Great Plains' use. Refining the training data used in the LULC classifications and masking wetlands can improve city-scale classification and enhance wetland delineation. We also recommend that the partners use stormwater flow analysis rather than HYDRAFloods to map flooding areas.

6. Acknowledgements

We would like to extend our gratitude to our partners at Audubon Great Plains, including Melissa Mosier (Platte River Program Manager), Joanna Grand (Director of Spatial Conservation Planning), and Zachary

Posnik (Spatial Ecologist for Spatial Conservation Planning), collaborator at University of Nebraska – Lincoln, Dr. Zhenghong Tang, and members of the DEVELOP Georgia – Athens Node, including Dr. Marguerite Madden (Science Advisor), Megan Rich (Center Lead), and Isabella Chittumuri, Shakirah Rogers, Nathan Tesfayi, & Nancee Uniyal (Georgia Disasters Fall 2022 DEVELOP Team). Additionally we appreciate deliverable feedback provided by Laramie Plott (DEVELOP Senior Fellow). We deeply appreciate all who have supported this project.

This material contains modified Copernicus Sentinel data (2019 – 2023) processed by ESA.

Any opinions, findings, conclusions, or recommendations expressed in this material are those of the authors and do not necessarily reflect the views of the National Aeronautics and Space Administration.
This material is based upon work supported by NASA through contract 80LARC23FA024.

7. Glossary

DEM – Digital elevation model

Earth observations – Satellites and sensors that collect information about the Earth's physical, chemical, and biological systems over space and time.

Edge Otsu Thresholding – An automatic threshold that combines Otsu's thresholding method with edge detection algorithms to determine the optimal threshold to separate foreground objects (edges) from the background in the image.

HAND – Height Above the Nearest Drainage

HYDRAFloods – Hydrologic Remote Sensing Analysis for Floods

JRC – Joint Research Centre

LULC – Land use land cover

MERIT – Multi-Error-Removed Improved-Terrain

ML – Machine Learning

MSI – Multispectral Instrument

NDVI – Normalized Difference Vegetation Index

NDBI – Normalized Difference Built-up Index

NDWI – Normalized Difference Water Index

NLCD – National Land Cover Database

Nature-based Solutions – Strategies that promote the use, enhancement, and restoration of natural elements to mitigate the impacts of climate change and provide environmental, economic, and social benefits (Kabisch et al., 2016).

OLI – Operational Land Imager

Random forest classification – An ensemble learning technique that constructs multiple decision trees during training. Each tree is trained on a random subset of the training data. The algorithm then aggregates the predictions from these trees through a majority vote to determine the final classification.

RGB – Red, green, and blue true color composite image

SAR – Synthetic Aperture Radar

8. References

Audubon Great Plains. (2023a). *Platte-Republican River Diversion.* https://greatplains.audubon.org/conservation/threats/water/platte-river

Audubon Great Plains. (2023b). *Platte River Initiative.* https://greatplains.audubon.org/node/922

Audubon Great Plains. (2023c). *Urban Woods and Prairies Initiative*. https://storymaps.arcgis.com/stories/1727e8812f314ca195c7fc350725c733

Birgé, H. E., Allen, C. R., Craig, R. K., & Twidwell, D. (2018). Resilience and Law in the Platte River Basin Social-Ecological System: Past, Present, and Future. In Cosens, B., Gunderson, L. (Eds.*), Practical Panarchy for Adaptive Water Governance*. Spring, Cham. https://doi.org/10.1007/978-3-319-72472-0_8

Breiman, Leo. 2001. "Random Forests." *Machine Learning 45*(1):5–32. doi: https://doi.org/10.1023/A:1010933404324.

Chittumuri, I., Rogers, S., Tesfayi, N., & Uniyal, N. (2022). *Georgia Disasters: Evaluating the Impacts of Hurricane Irma on Georgia Heirs' Property Owners Using NASA Earth Observations.* NASA NTRS. https://ntrs.nasa.gov/citations/20220016779

Conant, R. T., Kluck, D. R., Anderson, M. T., Badger, A. M., Boustead, B.M., Derner, J.D., Farris, L., Hayes, M.J., Livneh, B., McNeeley, S.M., Peck, D.E., Shulski, M.D., & Small, V. (2018). Chapter 22 : Northern Great Plains. Impacts, Risks, and Adaptation in the United States: The Fourth National Climate Assessment, Volume II. https://doi.org/10.7930/nca4.2018.ch22

Dewan, A. M. & Yamaguchi, Y. (2009). Land use and land cover change in Greater Dhaka, Bangladesh: Using remote sensing to promote sustainable urbanization. *Applied Geography, 29*, 390–401. https://doi.org/10.1016/j.apgeog.2008.12.005

Dewitz, J., and U.S. Geological Survey. (2021). National Land Cover Database (NLCD). 2019 Products (ver. 3.0, February 2024). U.S. Geological Survey data release. https://doi.org/10.5066/P9KZCM54.

European Space Agency: Copernicus Open Access Hub (2019). Sentinel 1 C-Synthetic Aperture Radar [Data set]. European Space Agency. https://sentinel.esa.int/web/sentinel/user-guides/sentinel-1-sar/

European Space Agency. Copernicus Open Access Hub (2017 – 2023). Sentinel 2A Multispectral Instrument (MSI) [Data set]. European Space Agency. https://sentinel.esa.int/web/sentinel/user-guides/sentinel-2-msi

Funk, C., Peterson, P., Landsfeld, M., Pedreros, D., Verdin, J., Shukla, S., Husak, G., Rowland, J., Harrison, L., Hoell, A., & Michaelsen, J. (2015). *CHIRPS Pentad: Climate Hazards Group Infrared Precipitation with*

Storm Data (Version 2.0). [Data set]. UCSB/CHG. Retrieved February 14, 2024, from https://doi.org/10.1038/sdata.2015.66

Gao, B. (1996). "NDWI—A Normalized Difference Water Index for Remote Sensing of Vegetation Liquid Water from Space." *Remote Sensing of Environment 58(*3), 257–66. https://doi.org/10.1016/S0034-4257(96)00067-3.

Kabisch, N., Frantzeskaki, N., Pauleit, S., Naumann, S., Davis, M., Artmann, M., Haase, D., Knapp, S., Horst, K., Stadler, J., Zaunberger, K., & Bonn, A. (2016). Nature-based solutions to climate change mitigation and adaptation in urban areas: perspectives on indicators, knowledge gaps, barriers, and opportunities for action. *Ecology and Society, 21*(2). http://dx.doi.org/10.5751/ES-08373-210239

Markert, K. N., Markert, A. M., Mayer, T., Nauman, C., Haag, A., Poortinga, A., Bhandari, B., Thwal, N.S., Kunlamai, T., Chishtie, F., Kwant, M., Phongsapan, K., Clinton, N., Towashiraporn, P., & Saah, D. (2020). Comparing Sentinel-1 surface water mapping algorithms and radiometric terrain correction processing in Southeast Asia utilizing Google Earth Engine. *Remote Sensing*, *12*(15), 2469. *MDPI AG*. http://dx.doi.org/10.3390/rs12152469

Pekel, J. F., Cottam, A., Gorelick, N., & Belward, A. S. (2016). High-resolution mapping of global surface water and its long-term changes. *Nature*, *540*, 418–422. https://doi.org/10.1038/nature20584

Rouse, J. W., R. H. Haas, J. A. Schell, and D. W. Deering. (1974). Monitoring Vegetation Systems in the Great Plains with ERTS. NASA NRTS. https://ntrs.nasa.gov/citations/19740022614

USDA Farm Production and Conservation - Business Center, Geospatial Enterprise Operations. (2019). National Agriculture Imagery Program [Dataset]. https://naip-usdaonline.hub.arcgis.com/.

U.S. Geological Survey, 3D Elevation Program 10-Meter Resolution Digital Elevation Model. (2023). [Dataset]. https://www.usgs.gov/3d-elevation-program.

U.S. Geological Survey Earth Resources Observations and Science Center (2018). Landsat 8 OLI/TIRS Level-2 Surface Reflectance. U.S. Geological Survey. Retrieved February 14, 2024, from https://www.usgs.gov/centers/eros/science/usgs-eros-archive-landsat-archives-landsat-8-olitirs-level-2-data-products

Velasquez, N., Quintero, F., Koya, S. R., Roy, T., & Mantilla, R. (2023). Snow-detonated floods: Assessment of the U.S. Midwest March 2019 event. *Journal of Hydrology: Regional Studies, 47*, 101387. https://doi.org/10.1016/j.ejrh.2023.101387

Vollrath, A., Mullissa, A., & Reiche, J. (2020). Angular-based radiometric slope correction for Sentinel-1 on Google Earth Engine. *Remote Sensing, 12*(11), 1867. https://doi.org/10.3390/rs12111867

Williams, C., Carey, L., De Los Santos, M., Fanelli, D., & Ireland, P. (2021). Central America Disasters: Using Earth Observations to Map Flooding for Disaster Monitoring, to Inform Potential Risk, and Prepare for Possible Response. [Unpublished manuscript]. NASA DEVELOP National Program, Alabama – Marshall. https://ntrs.nasa.gov/citations/20210026458

Yamazaki D., Ikeshima, D., Sosa, J., Bates, P. D., Allen, G. H., & Pavelsky, T. M. (2019). MERIT Hydro: A high-resolution global hydrography map based on latest topography datasets. *Water Resources Research*, *55*(6), 5053-5073, https://doi:10.1029/2019WR024873

Zha, Y., J. Gao, and S. Ni. (2003). Use of Normalized Difference Built-up Index in Automatically Mapping Urban Areas from TM Imagery. *International Journal of Remote Sensing 24*(3), 583–94. https://doi.org/10.1080/01431160304987.

9. Appendix

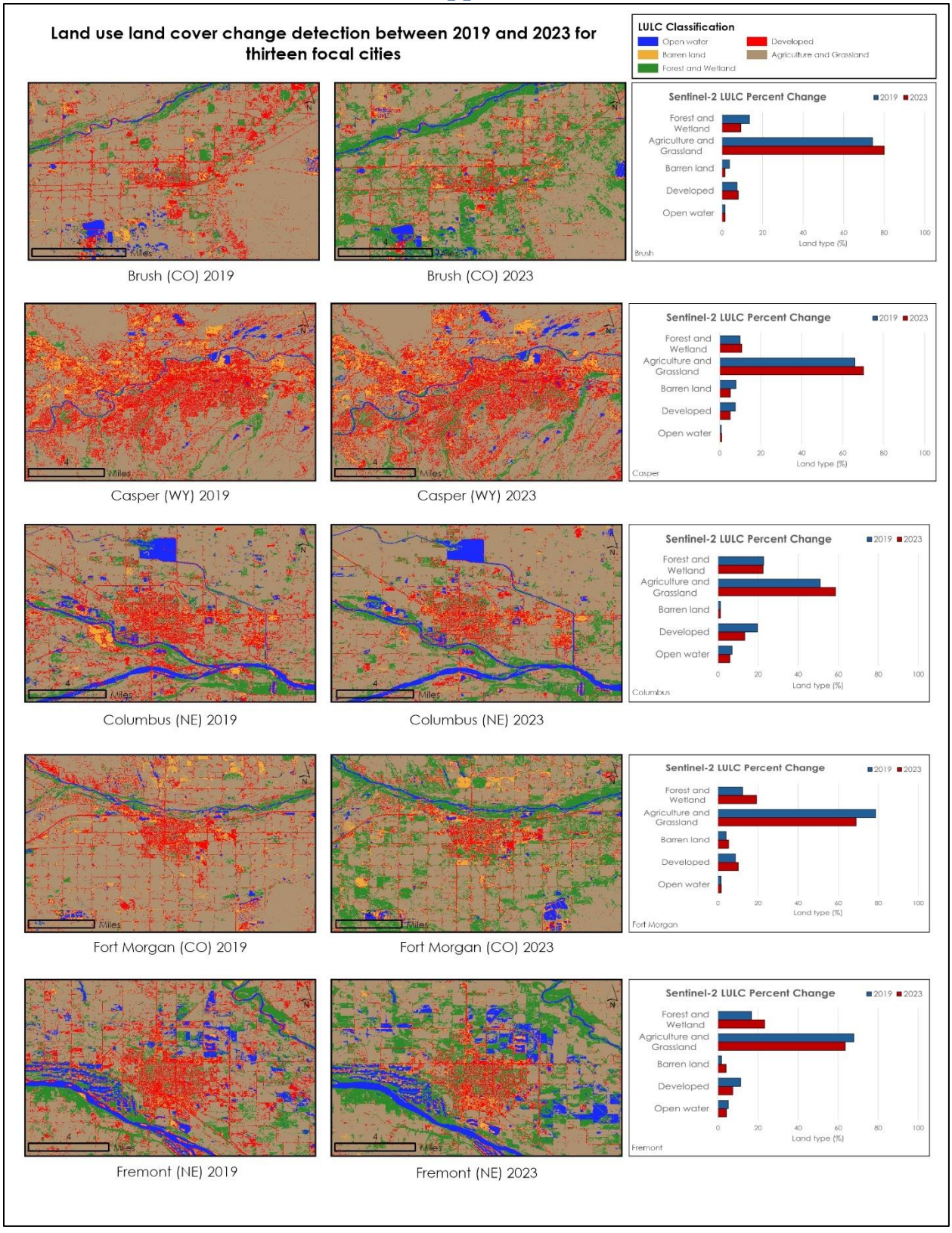
Land use land cover change detection between 2019 and 2023 for thirteen focal cities
LULC Classification
Open water
Developed
Barren land
Agriculture and Grassland
Forest and Wetland
Sentinel-2 LULC Percent Change
2019
2023
Forest and Wetland
Agriculture and Grassland
Barren land
Developed
Open water
Land type (%)
Brush
Brush (CO) 2019
Brush (CO) 2023
Casper
Casper (WY) 2019
Casper (WY) 2023
Columbus
Columbus (NE) 2019
Columbus (NE) 2023
Fort Morgan
Fort Morgan (CO) 2019
Fort Morgan (CO) 2023
Fremont
Fremont (NE) 2019
Fremont (NE) 2023

Land use land cover change detection: continued

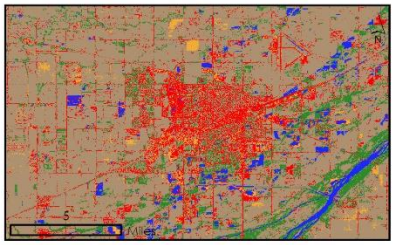

Grand Island (NE) 2019

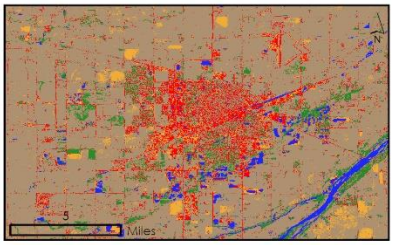

Grand Island (NE) 2023

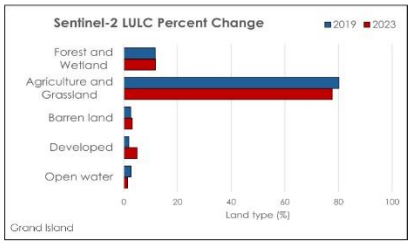

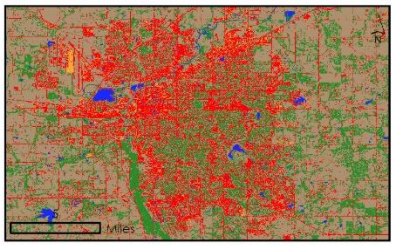

Lincoln (NE) 2019

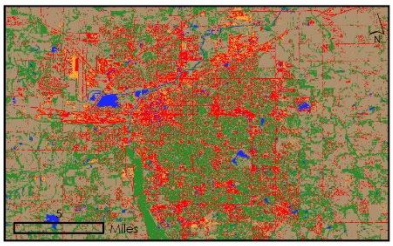

Lincoln (NE) 2023

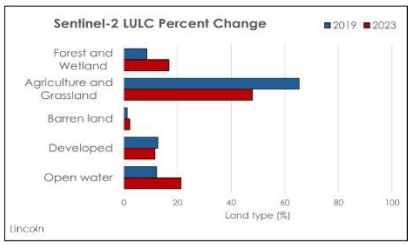

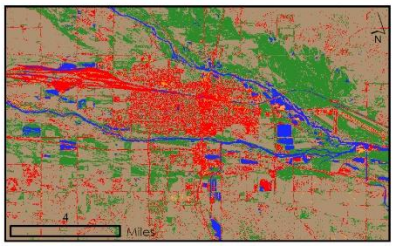

North Platte (NE) 2019

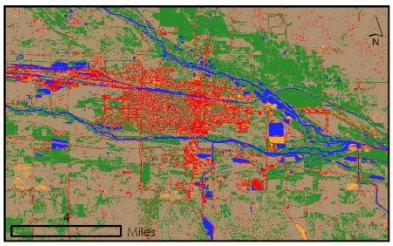

North Platte (NE) 2023

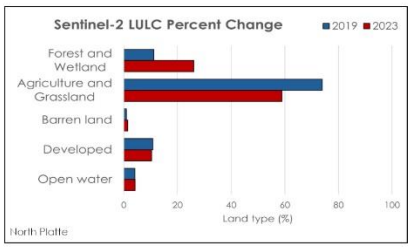

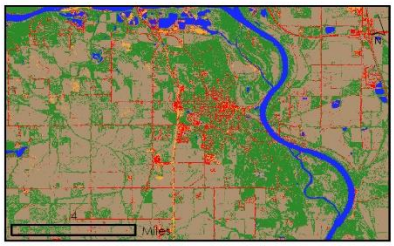

Plattsmouth (NE) 2019

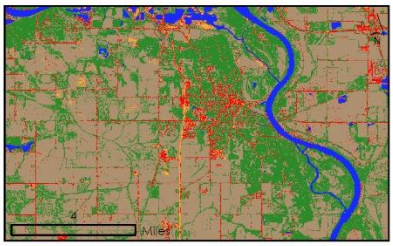

Plattsmouth (NE) 2023

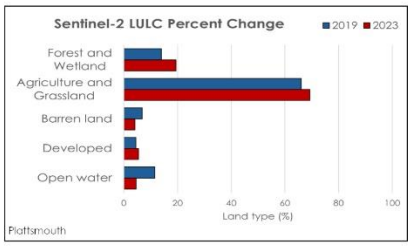

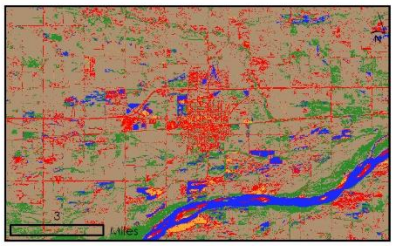

Schuyler (NE) 2019

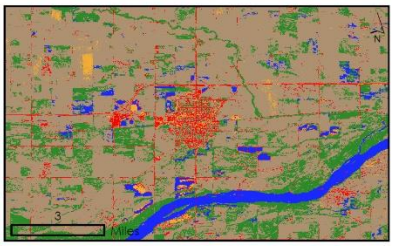

Schuyler (NE) 2023

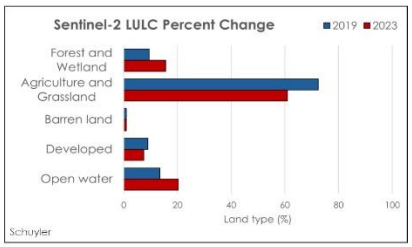

Figure A1. Land use land cover change detection within each of the thirteen focal cities.

Table A1.

Table of the LULC percent change within each of the thirteen focal cities.

+/- % Change by Focal City	Open Water	Developed	Forest and Wetlands	Barren Land	Agriculture and Grasslands
Brush	+6.63%	+8.65%	-32.34%	-58.397%	+7.83%
Casper	+33.62%	-33.39%	+9.1%	-35.12%	+6.32%
Columbus	-15.43%	-32.12%	-0.98%	-3.41%	+15.05%
Fort Morgan	+4.91%	+16.36%	+56.05%	+32.14%	-12.34%
Fremont	-16.85%	-34.05%	+39.47%	+131.31%	-6.24%
Grand Island	-46.22%	+170.46%	+0.78%	+22.27%	-3.16%
Lincoln	+74.77%	-8.36%	+97.34%	+79.38%	-26.583%
North Platte	+3.73%	-4.12%	+132.27%	+46.29%	-20.29%
Plattsmouth	-59.91%	+21.38%	+38.99%	-39.48%	+4.86%
Schuyler	+51.58%	-16.67%	+64.53%	-5.3%	-15.85%
Scottsbluff	+26.5%	-40.17%	+255.16%	+229.89%	-17.56%
Sterling	+129.25%	-32.33%	+11.13%	+31.36%	-5.94%
Torrington	+2.88%	-9.99%	+124.35%	+232.17%	-7.78%
Total	No Change	-33.33%	+33.33%	No Change	No Change